DMD Fast Forward. Published on April 13, 2015 as DOI: 10.1124/dmd.115.063388
This article has not been copyedited and formatted. The final version may differ from this version.

Hepatoselective NO-donors, V-PYRRO/NO and V-PROLI/NO in Nonalcoholic Fatty Liver Disease: a comparison of anti-steatotic effects with the biotransformation and pharmacokinetics

Kamil Kus, Maria Walczak, Edyta Maslak, Agnieszka Zakrzewska, Anna Gonciarz-Dytman, Piotr Zabielski, Barbara Sitek, Krystyna Wandzel, Agnieszka Kij, Adrian Chabowski, Ryan J. Holland, Joseph E. Saavedra, Larry. K. Keefer, Stefan Chlopicki

Jagiellonian Centre for Experimental Therapeutics (JCET), Jagiellonian University, Bobrzynskiego 14, 30-348 Krakow, Poland (K.K., M.W., E.M., A.Z., A.G.-D., B.S., K.W., A.K., S.Ch.)

Department of Pharmacokinetics and Physical Pharmacy, Jagiellonian University Medical College, Medyczna 9, 30-688 Krakow (K.K., M.W., A.G.-D., A.K.)

Department of Physiology, Medical University of Bialystok, Mickiewicza 2C, 15-222 Bialystok, Poland (P.Z., A.Ch.)

Leidos Biomedical Research, Inc., Frederick National Laboratory for Cancer Research, Frederick, Maryland 21702, United States (J.E.S.)

Chemical Biology Laboratory, National Cancer Institute, Frederick, Maryland 21702, United States (R.J.H., L.K.K.)

Department of Experimental Pharmacology, Chair of Pharmacology, Jagiellonian University, Medical College, Grzegorzecka 16, 31-531 Krakow, Poland (S.Ch.)

Running title:

Effects of two NO-donors on NAFLD and their ADME profiles

Corresponding author: Stefan Chlopicki

JCET Jagiellonian University.Ul. Bobrzynskiego 14

30-348 Krakow, Poland

e-mail: stefan.chlopicki.@jcet.eu

Number of text pages: 35

Number of tables: 1

Number of figures: 5

Number of references: 63

Number of words in Abstract: 247

Number of words in Introduction: 675

Number of words in Discussion: 1406

Abbreviations: NAFLD: nonalcoholic fatty liver disease; HFD: high fat diet; BSA: bovine serum albumin; TNF: tumor necrosis factor; cGMP: cyclic guanosine monophosphate ; eNOS: endothelial nitric oxide synthase; AUC: area under the curve; TAG: triacyloglicerole; TLC: thin-layer chromatography; FID: flame ionization detector; PUFA: polyunsaturated fatty acids; SFA: saturated fatty acids; PBS: phosphate-buffered saline; MRT: mean residence time; Cl: clearance; Vss: steady-state volume of distribution; E: hepatic extraction ratio; ALT: alanine aminotransferase; LDH: lactate dehydrogenase; CE/FA: capillary electrophoresis/frontal analysis; PDA: photodiode array detector; NADPH: nicotinamide adenine dinucleotide phosphate (reduced form); HPLC: high-performance liquid chromatography, GC: gas chromatography; K_M: Michaelis-Menten constant, V_{max}: maximal velocity.

DMD Fast Forward. Published on April 13, 2015 as DOI: 10.1124/dmd.115.063388
This article has not been copyedited and formatted. The final version may differ from this version.

Abstract

V-PYRRO/NO and V-PROLI/NO, two structurally similar diazeniumdiolate derivatives were designed as liver-selective prodrugs that are metabolized by cytochrome P450 izoenzymes, with subsequent release of nitric oxide (NO). Yet, their efficacy in the treatment of NAFLD (nonalcoholic fatty liver disease) and their comparative pharmacokinetic and metabolic profiles have not been characterized. The aim of the present work was to compare the effects of V-PYRRO/NO and V-PROLI/NO on liver steatosis, glucose tolerance and liver fatty acid composition in C57BL/6J mice fed a high fat diet (HFD) as well as to comprehensively characterize the ADME profiles of both these NO-donors. Despite their similar structure, V-PYRRO/NO and V-PROLI/NO showed differences in pharmacological efficacy in the murine model of NAFLD. V-PYRRO/NO, but not V-PROLI/NO attenuated liver steatosis, improved glucose tolerance and favorably modified fatty acid composition in the liver. Both compounds were characterized by rapid absorption following *i.p.* administration, rapid elimination from the body and incomplete bioavailability. However, V-PYRRO/NO was eliminated mainly by the liver, whereas V-PROLI/NO was excreted mostly in unchanged form by the kidney. V-PYRRO/NO was metabolized by CYP2E1, CYP2C9, CYP1A2 and CYP3A4, while V-PROLI/NO was metabolized mainly by CYP1A2. Importantly, V-PYRRO/NO was a better NO releaser *in vivo* and in the isolated, perfused liver than V-PROLI/NO, an effect compatible with the superior anti-steatotic activity of V-PYRRO/NO. In conclusion, V-PYRRO/NO displayed pronounced anti-steatotic effect associated with liver-targeted NO-release, while V-PROLI/NO showed low effectiveness, was not taken up by the liver and was eliminated mostly in unchanged form by the kidney.

Introduction

Many commonly used drugs do not possess biological activity *per se*, but are metabolized into active metabolites that exert a therapeutic effect. Increasing bioavailability, reducing toxicity, and achieving organ-selective delivery represent the major aims of prodrug development (Han & Amidon, 2000; Huttunen et al., 2008; Testa, 2009). One of the strategies for achieving hepato-selectivity in drugs is to develop prodrugs that are metabolized by specific enzymes in the liver (Erion et al., 2005; Han & Amidon, 2000; Zawilska et al., 2013). Since cytochrome P450-dependent enzymes represent a large family of enzymes responsible for metabolizing a vast number of xenobiotics, and are located mainly in the liver, they constitute an excellent target for liver-specific prodrugs (Huttunen et al., 2008; Ortiz de Montellano, 2013).

V-PYRRO/NO (O(2)-vinyl-1-(pyrrolidin-1-yl)diazen-1-ium-1,2-diolate) and V-PROLI/NO (O2-vinyl-[2-(carboxylato)pyrrolidin-1-yl]diazen-1-ium-1,2-diolate) (Fig. 1), are both diazeniumdiolates that were designed to deliver nitric oxide (NO) directly to the liver via cytochrome P450-dependent metabolism. The structure of these prodrugs was designed to avoid spontaneous decomposition under physiological conditions and, to facilitate cytochrome P450-related biotransformation into their respective epoxides. These unstable intermediates are formed in hepatocytes and hydrolyze, either spontaneously or via enzymatic reaction by hepatic epoxide hydrolase, to generate diazeniumdiolate ions, which spontaneously release NO (Saavedra et al., 1997). It has been demonstrated that V-PYRRO/NO metabolizes into biologically active NO in isolated hepatocytes but not in liver sinusoidal endothelial cells, Kupffer cells, arterial vascular smooth muscle cells, systemic endothelial cells, or murine macrophages, underscoring the hepatocytes selectivity of NO delivery by V-PYRRO/NO (Saavedra et al., 1997).

DMD Fast Forward. Published on April 13, 2015 as DOI: 10.1124/dmd.115.063388
This article has not been copyedited and formatted. The final version may differ from this version.

In turn, V-PROLI/NO is a novel proline-based analogue of V-PYRRO/NO with attached to the molecule additional carboxylic acid moiety to improve the water solubility. Furthermore, the additional functionality makes the major product of decomposition of V-PROLI/NO naturally occurring metabolite N-nitrosoproline, resulting in a favorable toxicological profile (Chakrapani et al., 2007; Hong et al., 2010).V-PYRRO/NO, on the other hand, is metabolized to N-nitrosopyrrolidine, which is burned with toxicity. To our knowledge, up to now, only one report has demonstrated that V-PROLI/NO is metabolized to NO in human hepatocytes, and in this report immortalized human HepG2 cells were used (Qu et al., 2010).

In turn, in numerous reports, V-PYRRO/NO has been shown to possess hepatoprotective effects, e.g. in TNF-α -induced hepatitis (Saavedra et al., 1997) or acetaminophen-induced toxicity (Liu et al., 2003), as well as in other *in vitro* and *in vivo* models of hepatocyte injury (DeLeve et al., 2003; Edwards et al., 2008; Gonget al., 2004; González et al., 2011; Holownia et al., 2009; Hu et al., 2013; Kim et al., 2000; Li et al., 2003; Liu & Waalkes, 2005; Liu et al., 2005; Liu et al., 2004; Liu et al., 2002; Qu et al., 2005, 2007; Ricciardi et al., 2001). Moreover, V-PYRRO/NO–derived NO release in the liver was shown to be followed by the elevation of liver cGMP with minimal systemic hypotensive effects (Saavedra et al., 1997). In contrast, hepatoprotective activity by V-PROLI/NO has only been reported in one study, which used the model of arsenic-induced toxicity in human HepG2 cells (Qu et al., 2010).

The evidence shows that NO regulates lipogenesis/lipolysis and controls gluconeogenesis/glycolysis pathways (Duplain et al., 2001; Ijaz et al., 2005; Jobgen et al., 2006). Over-expression of eNOS has consistently been demonstrated to protect against obesity, hyperinsulinemia, adipocyte hypertrophy, decreased plasma triglycerides and free fatty acid plasma concentration (Sansbury et al., 2012). On the other hand, impaired NO bioavailability has been shown to result in the development of hypertension, insulin resistance and obesity - being at

least in part a consequence of impaired fatty acid oxidation (Cook et al., 2003; Duplain et al., 2001; Gouill et al., 2007). Accordingly, liver-selective release of NO could represent an effective novel strategy for preventing liver steatosis and NAFLD. The aim of the present study was to compare the therapeutic effects of V-PYRRO/NO and V-PROLI/NO against HFD-induced liver steatosis and insulin resistance, as well as to comprehensively characterize the pharmacokinetic and metabolic profiles of these compounds in mice, with an attempt to find structural features of an effective liver-selective NO donor based on this comparison.

Material and Methods

Chemicals

Chemicals such as HPLC grade acetonitrile, formic acid and methanol were purchased from Merck (Darmstadt, Germany). Ketamine, heparin and isoflurane were bought from PGF Cefarm (Kraków, Poland). Xylazine, sodium chloride, calcium chloride, magnesium sulphate, sodium bicarbonate, potassium dihydrogen phosphate, glucose, pyruvic acid, EDTA, TRIS base, potassium chloride, sucrose, sodium phosphate dibasic, acetone, magnesium chloride, NADPH, Folin&Ciocalteu's phenyl reagent, potassium-sodium tartaretetrahydrate, copper sulphate, sodium hydroxide, phenacetin, acetaminophen, tolbutamide, 4-hydroxytolbutamide, bufuralol, 1-hydroxybufuralol, chlorzoxazone, 6-hydroxychlorzoxazone, midazolam, 1-hydroxymidazolam, 4-hydroxymidazolam, dextrorphan, furafylline, sulphaphenazole, (+)-N-3-benzylnirvanol, quinidine, disulfiram, and ketoconazole were purchased from Sigma-Aldrich (St. Louis, MO, USA). Water used in the study was prepared using a Milli-Q system (Millipore, Billerica, MA, USA).V-PYRRO/NO and V-PROLI/NO (>99% pure)were synthetized at the Center for Cancer

Research in the National Cancer Institute in Frederick, USA as described previously (Chakrapani et al., 2007; Saavedra et al., 1997).

Animals

Male C57BL/6J mice (16-25g) and Wistar rats (180-220g) were purchased from Charles River Laboratories (Raleigh, Germany). Animals were housed in colony cages in a room with constant temperature (21-25°C) a relative humidity of 40-65%, a standard light/dark cycle and access to food and water *ad libidum*. Prior to experiments, the animals were fasted overnight with free access to water. All procedures involving animals were conducted according to the Guidelines for Animal Care and Treatment of the European Union and were approved by the Local Ethical Committee for Experiments on Animals at the Jagiellonian University (Krakow, Poland).

Pharmacological study

Six-week old, male, C57BL/6J mice were fed a high fat diet (HFD; 60 kcal% of fat) (Research Diets, New Brunswick, NJ, USA) for 15 weeks. After 10 weeks of HFD feeding, treatment with V-PYRRO/NO at 5 mg/kg (32 μmol/kg *i.p.* bolus two times per day) or V-PROLI/NO at 6 mg/kg (29 μmol/kg *i.p.* bolus two times per day) was carried for an additional 5 weeks. At the end of the experiment, the animals were anesthetized with ketamine (100 mg/kg, *i.p.*) and xylazine (10 mg/kg *i.p.*).

Glucose tolerance test

For the glucose tolerance test, the mice were fasted for 4 h and then injected intraperitoneally with saturated glucose solution (at 2 g/kg of body weight). Blood was collected

from the tail veins prior to glucose administration (0 min) and at 15, 30, 45, 60 and 120 min following administration. Plasma glucose concentrations were measured by the enzymatic photometric method using an automatic biochemical analyzer Pentra 400 (Horiba, Kyoto, Japan) according to the manufacturer's instructions. Area under the curve (AUC) of blood glucose concentration versus time was calculated using the trapezoidal method.

Histological evaluation

Liver samples were fixed in 4% buffered formalin. Samples were embedded in OCT medium and frozen at -80°C, or prepared according to the standard paraffin method. OCT embedded 7 μm sections were stained with OilRed O for fat content examination. Paraffin embedded 5 μm sections were stained with hematoxylin and eosin for general histology and One step Gomorie's trichrome for fibrosis visualization. Sections were photographed at 100 x (OilRed O) and 200 x (H&E, One step Gomorie's trichrome) magnification with an Olympus BX51 light microscope (Olympus Corporation, Tokyo, Japan). Four images of each OilRed O stained section (n = 6/group) were analyzed for lipid content using the ImageJ software macro adapted for OilRed O staining.

Lipid analysis

Liver samples (ca. 100 mg) were powdered in a mortar precooled with liquid nitrogen followed by extraction of lipids in a chloroform-methanol solution. The fractions of triacylglycerols (TAG) were separated using thin-layer chromatography (TLC), according to the methodology of Baranowski et al. (Baranowski et al., 2013) and Zabielski et al. (Zabielski et al., 2010). Individual fatty acid methyl esters were liberated by acid methanolysis using BF_3MeOH, and were identified and quantified according to the retention times of standards by gas liquid

DMD Fast Forward. Published on April 13, 2015 as DOI: 10.1124/dmd.115.063388
This article has not been copyedited and formatted. The final version may differ from this version.

chromatography (Agilent 5890 Series II gas chromatograph with FID detector, Agilent CP-Sil88 capillary column, 50 m, 0.25 mm ID, 0.2 μm film; Agilent Technologies, Santa Clara, CA, USA). Total TAG content was estimated as the sum of the particular fatty acid species of the assessed fraction and expressed in nanomoles per gram of tissue. The content of saturated fatty acids (SFA, C14:0, C16:0, C18:0, C20:0, C22:0, C24:0), monounsaturated fatty acids (MUFA, C16:1, C18:1, C24:1) and polyunsaturated fatty acids (PUFA, 18:2 *n-6*, 18:3 *n-3*, 20:4 *n-6*, 22:6 *n-3*) in the TAG fractions were analyzed, along with PUFA/SFA ratio (Wierzbicki et al., 2009).

In vivo pharmacokinetics

The 6-week old male C57BL/6J mice were injected with V-PYRRO/NO or V-PROLI/NO as a single intravenous (*i.v.*) and intraperitoneal (*i.p.*) administration at a dose of 5 mg/kg (32 μmol/kg) or 6 mg/kg (29 μmol/kg) for V-PYRRO/NO and V-PROLI/NO, respectively. Animals were anesthetized with isoflurane at a concentration of 3-4% in 100% oxygen and sacrificed at the following time intervals: 0 (before dosing) and, 2, 5, 7, 10, 15, 20, 25, 30, 45, 60 90, 120 and 240 min after compounds administration. Blood samples were collected into heparinized microfuge tubes and centrifuged at 1000 rpm for 15 min. The plasma was separated into clean tubes and frozen at -20°C prior to analysis. The liver tissues were collected and rinsed with phosphate buffered saline (PBS, pH = 7.4) and stored at -80°C until analysis.

All data in the pharmacokinetic experiments were processed using the software Phoenix WinNonlin 6.3 (Certara, St. Louis, MO, USA). The non-compartmental approach was applied to calculate the basic pharmacokinetic parameters such as mean residence time (MRT), area under the curve (AUC), systemic clearance (Cl_T) and volume of distribution at steady-state (Vss).

Renal clearance

DMD Fast Forward. Published on April 13, 2015 as DOI: 10.1124/dmd.115.063388
This article has not been copyedited and formatted. The final version may differ from this version.

After a single *i.v.* injections of V-PYRRO/NO (5 mg/kg) or V-PROLI/NO (6 mg/kg), the 6-week old mice (n = 7) were individually placed in stainless steel metabolic cages for collection of urine. The urine samples were collected at 0-6, 6-12 and 12-24 h post dosing. The volumes of the urine samples were recorded and samples were stored at -20°C until analysis.

Renal elimination was assessed based on the fraction of administered dose excreted in the urine as unchanged form:

$$f_R = \frac{Ae^{\infty}}{D_{iv}} \qquad (1)$$

where f_R is a fraction of dose excreted by the kidney, Ae^{∞} is a total amount of studied substance in the urine and D_{iv} is the administered dose.

Renal clearance (Cl_R) of V-PYRRO/NO and V-PROLI/NO was calculated as follows:

$$Cl_R = f_R \times Cl_T \qquad (2)$$

$$Cl_R = \frac{Ae^{\infty}}{AUC_0^{\infty}} \qquad (3)$$

Hepatic extraction ratio

Hepatic elimination was determined using the *ex vivo* model of perfused mouse liver. Following *i.p.* injection of ketamine (100 mg/kg), xylazine (10 mg/kg) and 0.8 mg/kg of heparin, the vena porta and the vena cava inferior were cannulated and ligated, and the liver was perfused using U-100 system for organ perfusion (Hugo Sachs Electronik, Harvard Apparatus, March-Hugstetten, Germany) until effluent was blood-free. The liver was than excised and moved to a moist chamber. Perfusion was carried out with Krebs-Hanseleit buffer of the following composition: 118.0 mM NaCl, 2.52 mM $CaCl_2$, 1.16 mM $MgSO_4$, 24.88 mM $NaHCO_3$, 1.18 mM

DMD Fast Forward. Published on April 13, 2015 as DOI: 10.1124/dmd.115.063388
This article has not been copyedited and formatted. The final version may differ from this version.

KH_2PO_4, 4.7 mM KCl, 10.0 mM glucose, 2.0 mM pyruvic acid and 0.5 mM EDTA. After the initial stabilization period (15 min), either V-PYRRO/NO or V-PROLI/NO was added at a final concentration of 10 or 50 μM, respectively. The experiments were completed within 1 h after starting perfusion. The perfusion flow rate was 4.3 mL/min and samples were collected as follows: inlet samples every 20 min; and outlet effluents every 1 min, between 5 and 20 min, and then every 10 min. After the experiments, the livers were excised, dried and weighed.

To ensure the viability of the liver, alanine aminotransferase (ALT) and lactate dehydrogenase (LDH) activity in the effluents were measured every 15 min for the duration of the experiment by the enzymatic photometric method, using the automatic biochemical analyzer Pentra 400 (Horiba, Kyoto, Japan) according to the manufacturer's instructions.

A control experiment to exclude the binding of V-PYRRO/NO or V-PROLI/NO to the experimental set-up was conducted. For this purpose, buffer containing V-PYRRO/NO or V-PROLI/NO was perfused through the perfusion system without mounting of the isolated liver. Buffer samples were collected in the same way as in the experiments with the isolated liver.

The hepatic extraction ratio was calculated based on the V-PYRRO/NO and V-PROLI/NO concentrations in the inlet and outlet effluents:

$$E = \frac{C_{in} - C_{out}}{C_{in}} \qquad (4)$$

where E is the hepatic extraction ratio and C_{in} and C_{out} are concentrations of studied compounds in inlet or outlet liver effluent.

Protein binding

Binding of V-PYRRO/NO and V-PROLI/NO to bovine albumin (BSA) and α-acid glycoprotein (AGP) was determined using capillary electrophoresis in frontal analysis mode

DMD Fast Forward. Published on April 13, 2015 as DOI: 10.1124/dmd.115.063388
This article has not been copyedited and formatted. The final version may differ from this version.

(CE/FA) on a Beckman Coulter P/ACE MDQ CE system with a PDA detector fixed at 230 nm (Beckman Coulter, Brea, CA, USA). The working conditions were as follows: uncoated fused silica capillary length 60.2 cm (50 cm to the detector) with 50 µm ID and 360 µm OD; temperature of the capillary 37°C; applied voltage of 15 kV; observed currents of about 56 µA. Following the standard rinsing procedure, the samples were injected at 0.5 psi for 40 s (injected sample volume represented 5% of total capillary volume). The unbound concentrations of V-PYRRO/NO and V-PROLI/NO were determined by comparing the plateau peak height of the equilibrated samples with the peak height of V-PYRRO/NO or V-PROLI/NO in the absence of BSA or AGP.

The results were expressed as the saturation fraction (*r*), representing the number of moles of compound bound (C_b) per mole of protein (*P*):

$$r = \frac{C_b}{P} \qquad (5)$$

The percent of binding was determined using Equation 6:

$$\%\ bound = \frac{C_t - C_u}{C_t}\ x\,100 \qquad (6)$$

where C_t is the total concentration of compound in the protein solution, and C_u is the free analyte concentration.

The equilibrium association constant (K_a) in the binding class (*m*) and the number of binding sites (*n*) were determined by a non-linear regression analysis using Wolfram Matematica 8.0 software (La Jolla, CA, USA) to fit the data to Equation 7:

$$r = \sum_{i=1}^{m} \frac{n_i \cdot C_u}{K_{di} + C_u} \qquad (7)$$

DMD Fast Forward. Published on April 13, 2015 as DOI: 10.1124/dmd.115.063388
This article has not been copyedited and formatted. The final version may differ from this version.

where *r* is the number of moles of drug bound per mole of protein (*Cb/Pt*; where *Pt* is the total protein concentration); *m* is the number of independent classes of binding sites; K_{di} is the dissociation constant for the i-th class and n_i is the number of binding sites in the i-th class.

In vitro metabolism by CYP450

Rats were sacrificed by decapitation and liver microsomes were prepared by differential centrifugation. Briefly, liver fragments were washed with 20 mM TRIS/KCl buffer (pH = 7.4) and homogenized (IKA-Werke GmbH & Co. KG Staufen, Janke, Germany). The homogenate was centrifuged (Sorval WX Ultra Series, Thermo Scientific, Waltham, MA, USA) at approximately 11,500 x g for 20 min at 4°C. The supernatant (S9 fraction) was transferred to new tubes and centrifuged at 100,000 x g for 1 h at 4°C. The pellet was suspended in 0.15 M KCl and centrifuged again at 100,000 x g for 1 h at 4°C. The obtained pellet was dispersed in TRIS/sucrose buffer and stored at -80°C until use. Protein concentration in the microsomal fraction was determined by Lowry protein assay (Lowry et al., 1951).

V-PYRRO/NO or V-PROLI/NO at the concentration range of 0.5-50 µM was incubated with the rat liver microsomes (1 mg/mL) in 0.1 M phosphate buffer (pH = 7.4) containing 10 mM $MgCl_2$. After 5 min of preincubation at 37°C, the incubation reactions were initiated with the addition of NADPH to a final concentration of 1 mM and were stopped after 20 min by placing samples on ice and adding ice-cold acetonitrile containing internal standard (4-hydroxymephenytoin at a concentration of 20 ng/mL). Basic kinetic parameters, Vmax and Km for V-PYRRO/NO and V-PROLI/NO, were calculated with GraphPad Prism 6.02 software (La Jolla, CA, USA) using nonlinear regression.

To test the involvement of cytochrome P450 isoenzymes in V-PYRRO/NO and V-PROLI/NO metabolism the following cytochrome P450-dependent isoenzymes inhibitors were

DMD Fast Forward. Published on April 13, 2015 as DOI: 10.1124/dmd.115.063388
This article has not been copyedited and formatted. The final version may differ from this version.

used: furafylline (1.5 µg/mL) for CYP1A2, sulfaphenazole (15 µg/mL) for CYP2C9, (+)-N-3-benzylnirvanol (1 µg/mL) for CYP2C19, quinidine (15 µg/mL) for CYP2D6, disulfiram (15 µg/mL) for CYP2E1 and ketoconazole (5 µg/mL) for CYP3A4.

To study the effects of V-PYRRO/NO and V-PROLI/NO on cytochrome P450 isoenzymes activity, a 'cocktail' method was used based on measurement of the concentration of metabolites derived from CYP450 isoenzymes-specific substrates. Briefly, V-PYRRO/NO or V-PROLI/NO, in the concentration range of 0.1 µM - 1 mM was incubated with rat liver microsomes suspended in 0.1 M phosphate buffer (pH 7.4), 10 mM $MgCl_2$, and substrate cocktail, at concentrations near their Km values: phenacetin (7.5 µg/mL) for CYP1A2; tolbutamide (2.5 µg/mL) for CYP2C9; bufuralol (12.5 µg/mL) for CYP2D6; chlorzoxazone (12.5 µg/mL) for CYP2E1, and midazolam (7 µg/mL) for CYP3A4. After addition of V-PYRRO/NO or V-PROLI/NO, the reaction mixtures were preincubated for 5 min at +37°C in a shaking water bath (Grant Instruments, Royston, UK) and next the reaction was initiated by addition of 1 mM NADPH. Following a 10 min incubation, the reaction was terminated with an ice-cold mixture of acetonitrile: acetone (1:1; v/v) containing the internal standard dextrorphan (50ng/mL). Samples were subsequently cooled on ice for 20 min to precipitate the protein, and then centrifuged at approximately 15,000 x g for 15 min at 4°C. The supernatant was analyzed immediately after incubation.

Chromatographic and mass spectrometric analysis

V-PYRRO/NO and V-PROLI/NO concentrations in plasma, liver homogenates, urine, liver effluents and in the incubation mixture of microsomes (50 µL) were measured after deproteinization using ice-cold acetonitrile (500 µL) containing internal standard (4-hydroxymephenytoin, 20 ng/mL). Samples were subsequently cooled on ice for 20 min to

DMD Fast Forward. Published on April 13, 2015 as DOI: 10.1124/dmd.115.063388
This article has not been copyedited and formatted. The final version may differ from this version.

precipitate the protein and then centrifuged at approximately 15,000 x g for 15 min at 4°C. The supernatant was transferred to an HPLC vial, and 5 µL volume was injected onto the analytical column. The analytical system consisted of UFLC Nexera (Shimadzu, Kyoto, Japan) coupled with a QTrap 5500 mass spectrometer (ABSciex, Framingham, MA, USA). Chromatographic separation was achieved using the Acquity UPLC BEH C18 (1.7 µm, 3.0 x 100 mm, Waters, Milford, MA, USA) analytical column, with acetonitrile and water containing 0.1% formic acid in the isocratic elution (45:55 v/v), at a flow rate of 0.4 mL/min. The analyzed compounds were detected in positive ionization MRM mode, monitoring the transitions of protonated ions m/z 158→70 for V-PYRRO/NO, m/z 202→100 for V-PROLI/NO and m/z 235→150 for IS. The operating conditions were as follows: curtain gas 20 psi, ion spray voltage 5000 V, temperature 400°C, ion source gases 1 50 psi and ion source gases 2 15 psi. Nitrogen was used as the curtain and collision gas.

Chromatographic separation of the metabolites of model CYP450 substrates was performed on a Kinetex analytical column (2.6 µm PFP 100 Å, 3 mm x 100, Phenomenex, Torrence, CA, USA) using an Ultimate 3000 UPLC system (Dionex, Sunnyvale, CA, USA). The mobile phase consisted of acetonitrile containing 0.1% formic acid (eluent A) and water containing 0.1% formic acid (eluent B). At a flow rate of 500 µL/min, the amount of eluent A was increased linearly from 20 to 95% over 2 min, was maintained at 95% for 6 min, returned to 20% over 3 min and left to re-equilibrate for 6 min. The total run time was 15 min. The analytes were detected using a TSQ Quantum Ultra triple quadrupole mass spectrometer (Thermo Scientific, Waltham, MA, USA). Heated electrospray ionization (H-ESI) was used in both positive and negative mode (for 6-hydroxychlorzoxazone). The selected reaction monitoring (SRM) transitions for each quantified substance and the internal standard were as follows: acetaminophen m/z 152→110, 4-hydroxytolbutamide m/z 287→89, 4-hydroxymephenytoin m/z

235→150, 1-hydroxybufuralol m/z 278→186, 6-hydroxychlorzoxazone m/z 184→120, 1-hydroxymidazolam m/z 342→324, 4-hydroxymidazolam m/z 342→297 and dextrorphan (IS) m/z 258→157. The operating conditions were as follows: needle voltage 4020 V, vaporizer temperature 250°C, sheath gas (nitrogen) pressure 30 psi, auxiliary gas (nitrogen) pressure 10 psi, capillary temperature 370°C. The argon gas pressure in the collision cell was approximately 2 mTorr.

Nitrite and nitrate measurements

The plasma samples were precipitated with methanol in the ratio of 1:1 (v/v). Liver samples were homogenized with methanol 1:2 (w/v). Following centrifugation at 10,000 x g for 10 min 10 µL of supernatant was injected onto the separation column.

The concentrations of nitrite and nitrate were measured by the NOx analysis system, ENO-20 (Eicom, Kyoto, Japan), based on the liquid chromatography method with post-column derivatization with Griess reagent. Nitrite and nitrate were separated on a NO-PAK column (4.6 x 50 mm, Eicom, Kyoto, Japan). Nitrate was reduced to nitrite by a cadmium-copper column (NO-RED, Eicom, Japan). Nitrite was detected based on the Griess reaction, with sulfanilamide and naphthylethylenediamine forming a purple diazo compound with the absorbance of dye product measured at 540 nm. The flow of the mobile phase (Carrier solution, Eicom, Kyoto, Japan) was 0.33 mL/min. The Griess reagent was delivered at a flow rate of 0.11 mL/min.

Statistical analysis

Data are expressed as mean ± SEM. The assessment of normality and heterogenity of variances was performed using the Shapiro-Wilk test and Flinger-Killeen test, respectively. To assess the statistical significance of the pharmacokinetics results, a Student's t-test and the nonparametric Mann-Whitney test were used. For pharmacological experiments, the

nonparametric Kruskal-Wallis test or one-way analysis of variance (ANOVA) and Tukey post-hoc test were used. The results were analyzed using Statistica 10.0 software (Statsoft, Tulsa, OK, USA).

Results

Effects of V-PYRRO/NO and V-PROLI/NO treatment on NAFLD

Treatment with V-PYRRO/NO, but not V-PROLI/NO, attenuated liver steatosis as evidenced by histopathological analysis (Figs. 2A, B, C) with semi-automatic quantitative analysis of liver fat content based on OilRed O stained slides (Fig. 2D), as well as by liver triglyceride content based on GC-FID chromatography (Fig. 2E). Furthermore, V-PYRRO/NO, but not V-PROLI/NO favorably changed fatty acid composition by increasing the PUFA/SFA ratio in mice fed with HFD (Fig. 2F). Finally, the overall glucose exposure, calculated on the basis of area under the curve (AUC) of blood glucose concentration versus time on the tolerance chart was significantly improved in V-PYRRO/NO-treated mice, while there was no improvement seen in V-PROLI/NO-treated mice (Figs. 2G, H).

Pharmacokinetic profile of V-PYRRO/NO and V-PROLI/NO

The mean plasma concentrations versus time profiles of V-PYRRO/NO and V-PROLI/NO after *i.v.* and *i.p*. administration are depicted in Fig. 3A. and the pharmacokinetic parameters are given in Table 1.

V-PYRRO/NO was eliminated more rapidly than V-PROLI/NO, as evidenced by a lower MRT and higher clearance values. V-PYRRO/NO was detectable in plasma for up to 60 min after

i.v. administration and 30 min after *i.p.* administration, respectively, whereas V-PROLI/NO was measurable over the entire sampling period. Moreover, V-PYRRO/NO was widely distributed in the intra- and extracellular water (Vd_{ss} = 0.88 L/kg), while V-PROLI/NO distribution was limited to the extracellular fluid (Vd_{ss} = 0.15 L/kg). In view of the fact that the pharmacological effects were studied following intraperitoneal administration of V-PYRRO/NO and V-PROLI/NO, pharmacokinetic studies following *i.p.* dosing were also conducted. Both compounds were rapidly absorbed after *i.p.* administration, with lower bioavailability for V-PYRRO/NO as compared to V-PROLI/NO (about 28% and 51%, respectively).Systemic NO release following *i.v.* administration of V-PYRRO/NO was higher than with V-PROLI/NO, as evidenced by nitrate and nitrite plasma concentrations (Figs. 3B, C).

Hepatic metabolism of V-PYRRO/NO and V-PROLI/NO

To assess the liver disposition of V-PYRRO/NO and V-PROLI/NO, the concentration of each compound in liver homogenates was measured following *i.v.* or *i.p.* administration of the compounds. V-PYRRO/NO was not detectable, while V-PROLI/NO was distributed in the liver, with maximum concentrations of 35.8 nmol/g (tmax = 2 min) and 23.9 nmol/g (tmax = 7 min) following *i.v.* and *i.p.* administration, respectively. Even after 60 min, the concentration of V-PROLI/NO remained elevated (5.3 nmol/g and 2.5 nmol/g after *i.v.* and *i.p.*, respectively).

To compare the decomposition of V-PYRRO/NO and V-PROLI/NO in the liver in greater detail, the uptake and metabolism of these analogs were studied in the isolated, perfused mouse liver set-up. V-PYRRO/NO exhibited nonspecific binding to the experimental set-up, resulting in a 25% decrease in the introduced dose to the liver that was included in the calculations of the hepatic extraction ratio, whereas binding of V-PROLI/NO to perfusion set-up was not significant. As shown in Figs. 4 A and 4 B the concentrations of V-PYRRO/NO in the liver effluents

DMD Fast Forward. Published on April 13, 2015 as DOI: 10.1124/dmd.115.063388
This article has not been copyedited and formatted. The final version may differ from this version.

amounted to about 70% of the initial concentration, taking into account the binding to experimental set-up; therefore, the calculated hepatic extraction ratio was about 0.3, and the hepatic clearance was 0.058 L/min/kg. In contrast, V-PROLI/NO was hardly metabolized in the liver, with outflow concentrations of the compound near its inflow concentration. The hepatic extraction ratio for V-PROLI/NO was below 0.1 (about 0.05) and hepatic clearance was 0.0005 mL/min/kg, suggesting negligible liver metabolism of V-PROLI/NO, in contrast with V-PYRRO/NO. These findings were confirmed by the measurements of concentrations of nitrite and nitrate in the liver samples after a one-hour perfusion of V-PYRRO/NO or V-PROLI/NO at the concentration of 50 μM. V-PYRRO/NO perfusion resulted in elevations in nitrite and nitrate liver content by over two fold (NO_2^-: 4.8 nmol/g and NO_3^-: 23.3 nmol/g), while V-PROLI/NO perfusion did not increase nitrite or nitrate concentration in the liver homogenate (NO_2^-: 1.7 nmol/g and NO_3^-: 13.4 nmol/g). Altogether, these results confirm considerable liver metabolism of V-PYRRO/NO, with subsequent NO release, but not of V-PROLI/NO.

Renal elimination of V-PYRRO/NO and V-PROLI/NO

As shown in Fig. 4C, less than 0.1% of V-PYRRO/NO was eliminated in the urine, while approximately 61% of V-PROLI/NO was excreted in the urine as unmodified compound. The calculated renal clearance for V-PYRRO/NO was very low and without physiological significance, while the renal clearance for V-PROLI/NO was significantly higher and amounted to 0.0032 L/min/kg.

Protein binding of V-PYRRO/NO and V-PROLI/NO

Both analogs bound to BSA with one class of binding site, and percent of binding amounting to 25.13 ± 4.5% and 53.33 ± 7.1% for V-PYRRO/NO and V-PROLI/NO, respectively. However, binding affinity to BSA was relatively low ($K_a = 1.93 \times 10^3$ M^{-1} and 7.57

DMD Fast Forward. Published on April 13, 2015 as DOI: 10.1124/dmd.115.063388
This article has not been copyedited and formatted. The final version may differ from this version.

$\times 10^3$ M^{-1}, for V-PYRRO/NO and V-PROLI/NO, respectively). Binding of studied analogs to AGP was also very low and not of physiological significance (3.15 ± 2.9 and 3.05 ± 1.43 for V-PYRRO/NO and V-PROLI/NO, respectively), probably due to the acidic character of these molecules.

Role of cytochrome P450 in V-PYRRO/NO and V-PROLI/NO metabolism

The calculated kinetic parameters derived using the Michaelis–Menten transformation (Fig. 5A) for V-PYRRO/NO were Km = 131.6 ± 38.15 μM and Vmax = 6.35 ± 1.41 μmol/min/mg protein. Based on the kinetic plots, V-PROLI/NO seems to have a low affinity for the cytochrome P450 isoenzymes. The Eadee-Hofstee plots were non-linear suggesting multiple-enzyme catalysis (data not shown).

The effect of selective CYP450 inhibitors on the biotransformation of V-PYRRO/NO and V-PROLI/NO using isoenzyme selective chemical inhibitors is shown in Fig. 5B. As evidenced by the effects of their respective inhibitors, V-PYRRO/NO was metabolized mainly by CYP2E1, but also by CYP2C9, CYP1A2 and CYP3A4, while V-PROLI/NO was biotransformed mainly by CYP1A2 and CYP2C9.

Neither V-PYRRO/NO nor V-PROLI/NO inhibited CYP450 isoenzymes as evidenced by the lack of inhibition of phenacetin-*O*-deetylation (CYP1A2), tolbutamide-4-hydroxylation (CYP2C9), bufuralol-1-hydroxylation (CYP2D6), chlorzoxazone-6-hydroxylation (CYP2E1) and midazolam-1- and -4-hydroxylation (CYP3A4), up to a concentration of 1 mM V-PYRRO/NO and V-PROLI/NO (data not shown).

Discussion

In the present study we compared two NO-donors (V-PYRRO/NO and V-PROLI/NO) that were designed to deliver nitric oxide to the liver via cytochrome P450-dependent metabolism, by looking at their effects on liver steatosis, liver fatty acid composition and insulin resistance, and comprehensively analyzing their pharmacokinetics and metabolism profiles. In the study we demonstrated that despite having similar chemical structures, only V-PYRRO/NO attenuated liver steatosis, increased liver PUFA/SFA ratio and improved postprandial glucose tolerance, while V-PROLI/NO was ineffective in these tests. Pharmacokinetic studies revealed rapid absorption following *i.p.* administration, intense elimination and incomplete bioavailability for both V-PYRRO/NO and V-PROLI/NO. However, it was noticed that V-PYRRO/NO was metabolized in the liver by CYP2E1, CYP2C9 and CYP3A4, while V-PROLI/NO was eliminated mostly in unchanged form by the kidney. Importantly, V-PYRRO/NO proved to be a better NO releaser in the mouse *in vivo* and in the isolated liver as compared with V-PROLI/NO, and results were consistent with superior anti-steatotic activity for V-PYRRO/NO. In conclusion, we provide clear-cut evidence that V-PYRRO/NO displays pronounced anti-steatotic effect associated with liver-targeted NO release, while V-PROLI/NO is not effective, is not taken up by the liver and is eliminated mostly unchanged by the kidney.

In physiological conditions nitric oxide generated mainly by eNOS (Förstermann & Sessa, 2012) plays a crucial role in liver homeostasis. NO activates soluble guanyl cyclase (sGC), which activates cGMP-dependent protein kinase (Pfeifer et al., 2013) and its role is not limited to the regulation of hepatic arterial resistance (Rockey & Shah, 2004). In fact, NO/cGMP–dependent signaling pathway exerts an anti-inflammatory and anti-fibrotic effect by limiting Kupffer cells and hepatic stellate cells activation (Tateya et al., 2011). NO also inhibits caspase activation, and therefore apoptosis, in hepatocytes (Kim et al., 2000). Furthermore, the remarkable regenerative ability of the liver is linked to NO activity (Carnovale & Ronco, 2012).

NO is also a regulator of glucose and lipid metabolism (Jobgen et al., 2006), it decreases fatty acid storage by improving their catabolism, and it attenuates *de novo* fatty acid synthesis. Moreover, NO regulates glucose metabolism by increasing glucose transport and metabolism as well as inhibiting gluconeogenesis and glycogen deposition (Jobgen et al., 2006).

Clearly, inadequate NO production by liver sinusoidal endothelial cells results in unopposed hepatic stellate cells activation and promotion of liver inflammation, which may contribute to the progression of portal hypertension (Hu et al., 2013), sinusoidal obstruction syndrome (SOS) (DeLeve, 2008), ischemia-reperfusion injury (Siriussawakul, 2010) and liver steatosis (Maslak et al, 2015). In fact, impairment of the NO signaling resulted in decreased glucose uptake, fasting hyperglycemia and the development of insulin resistance (An et al., 2012; Lutz et al., 2011).

In line with the importance of NO in the maintenance of metabolic homeostasis,the beneficial effect of NO-based therapy has been demonstrated in obesity (Jobgen et al., 2009), insulin resistance (Sadri & Lautt, 1999) and liver steatosis (de Oliveira et al., 2006). However, in contrast to the present paper, none of these reports concerned the direct delivery of NO to the liver (Ricardo et al., 2002). In the current study we aimed at comparing the anti-steatotic efficacy of two structurally related hepatocyte-specific NO-donors, and revealed a hepato-specific, and hepato-protective action of V-PYRRO/NO, but not of V-PROLI/NO, against NAFLD. Moreover, the liver-specific effects of V-PYRRO/NO-derived NO release not only attenuated liver steatosis, but were also associated with changes in fatty acid composition, in particular the amelioration of the PUFA/SFA ratio, most likely due to inhibition of endogenous fatty acid synthesis. Our findings are of particular importance because fatty acid saturation has been shown to be involved in the pathogenesis of insulin resistance (van den Berg et al., 2010) and metabolic syndrome (Warensjö et al, 2005). In fact, in our previous work, we demonstrated that the effect of V-

DMD Fast Forward. Published on April 13, 2015 as DOI: 10.1124/dmd.115.063388
This article has not been copyedited and formatted. The final version may differ from this version.

PYRRO/NO on insulin resistance and steatosis was mediated by NO-dependent Akt activation and inhibition of *de novo* fatty acid synthesis by ACC phosphorylation (Maslak et al., 2015). Interestingly, despite previously reported data, indicating NO release *in vitro* (Hong et al., 2010) and favorable toxicity (Chakrapani et al., 2007) V-PROLI/NO did not influence insulin resistance and fatty acid composition in mice in the present study.

The superior pharmacological activity of V-PYRRO/NO was not associated with higher bioavailability than V-PROLI/NO following *i.p.* administration. In fact, V-PROLI/NO showed greater bioavailability (51%) than V-PYRRO/NO (27%). Similar results for the bioavailability of V-PYRRO/NO were reported by Stinson et al. (Stinson et al., 2002). The incomplete bioavailability, besides the first-pass effect, might be a result of extrahepatic metabolism of V-PYRRO/NO and V-PROLI/NO, since the cytochrome P450 enzyme system is also located in other extrahepatic tissues, including the lungs, kidneys and small intestine (Ding & Kaminsky, 2003; Nebert & Russell, 2002; Paine et al., 2006; Pavek & Dvorak, 2008; Peter, 1992). Partial decomposition of V-PYRRO/NO and V-PROLI/NO in other organs may explain the increased nitrite and nitrate plasma concentrations detected following *i.v.* administration of the compounds. However, we are confident that even though V-PYRRO/NO was partially metabolized in extrahepatic tissues, its pharmacological effect came mostly, if not entirely, from liver-specific NO release.

The results from the specific cytochrome P450 inhibitors demonstrated that V-PYRRO/NO was mainly a substrate for CYP2E1, as well as for CYP1A2, CYP2C9 and CYP3A4, while V-PROLI/NO was shown to be metabolized mainly by CYP1A2 and CYP2C9 in the liver. These results are partially in line with the findings of Inami et al. (Inami et al., 2006), who showed that CYP2E1, CYP2A6 and CYP2B6 are responsible for V-PYRRO/NO metabolism in human liver microsomes. On the other hand V-PROLI/NO, was metabolized

mainly by CYP1A2 and to a lesser extent by CYP2E1 and CYP3A4, as reported previously (Chakrapani et al., 2007), but with low enzyme affinity.

Increased metabolism and NO production in V-PROLI/NO-treated HepG2 cells, as compared with V-PYRRO/NO treatment was previously demonstrated by Hong et al. (2010). However, high concentrations of V-PYRRO/NO and V-PROLI/NO were required to generate relatively low concentrations of nitrite (reported by Hong et al. 2010 and confirmed by us, unpublished results), suggesting a relatively low biotransformation of the compounds in HepG2 cells. This notion seems to be in line with recent studies showing that in human hepatoma cells (e.g. HepG2), the expression of most of CYP 450 izoenzymes is substantially reduced as compared with primary human hepatocytes (about 100 to 1000-fold lower) (Lin et al., 2012; Pawłowska & Augustin, 2011; Westerink & Schoonen, 2007). Moreover, in HepG2 cell lines, the activity of CYP 450 enzymes are much lower than in *ex vivo* isolated primary hepatocytes (Lin et al., 2012; Westerink & Schoonen, 2007). Additionally, since the expression and activity of CYP1A2 is higher than that of CYP2E1 in HepG2 cells (Westerink & Schoonen, 2007), Hong et al. (2010) found high release of NO from V-PROLI/NO, as compared to V-PYRRO/NO. In our hands, biotransformation of V-PROLI/NO was dependent on CYP1A2 and CYP2C9, while V-PYRRO/NO mainly on CYP2E1. This is not surprising that Gong et al. (2004) demonstrated that HepG2 cells failed to generate nitrite and nitrate from V-PYRRO/NO. Accordingly, we believe that the HepG2 cell line used as a model system to study NO release from V-PYRRO/NO and V-PROLI/NO is not relevant to primary hepatocytes or the *in vivo* setting, thus giving contradictory results from our present study, which was performed *in vivo* and in *ex vivo* isolated liver set-up.

In the present work, we also demonstrated, that the differences in the plasma pharmacokinetic profiles of V-PYRRO/NO and V-PROLI/NO may be linked to differences in their lipophilicity caused by an additional carboxylic acid moiety in V-PROLI/NO's structure. *In*

DMD Fast Forward. Published on April 13, 2015 as DOI: 10.1124/dmd.115.063388
This article has not been copyedited and formatted. The final version may differ from this version.

silico predicted logP values for both analogs differed from -1.63 to 1.01 for V-PYRRO/NO and from -3.92 to -2.76 for V-PROLI/NO depending on the pH of the environment. V-PYRRO/NO, being more lipophilic, was widely distributed in the total body water (Vd_{ss} = 0.88 L/kg), while V-PROLI/NO distribution was limited only to the extracellular fluid (Vd_{ss} = 0.149 L/kg). Differences in PK profiles can be also related to the participation of. proline transporters in the case of V-PROLI/NO but not of V-PYRRO/NO.

Moreover, the results showed that the affinity of V-PYRRO/NO and V-PROLI/NO to BSA was rather low. V-PROLI/NO was bound to BSA to a greater extent, probably due to the stronger acidic character, which can partially explain its slower elimination and longer biological half-life. Furthermore, we provide evidence that neither compounds affects the activity of cytochrome P450, as shown in the direct inhibition study. In summary, both analogs display distinct CYP450 metabolism, distinct pharmacokinetic profile, and differences in renal excretion.

Conclusions

In summary V-PYRRO/NO but not V-PROLI/NO protected against HFD-induced liver steatosis and improved insulin resistance in mice fed a high fat diet. The compounds' distinct pharmacological effects can be explained by their pharmacokinetic and metabolic profiles. V-PYRRO/NO displayed a pronounced anti-steatotic effect associated with liver-targeted NO release, while V-PROLI/NO was ineffective, not taken up by the liver and was eliminated mostly unchanged by the kidney. It is worth to add, that therapy with liver targeted NO-donors, free of systemic hypotensive effects, represents a promising therapeutic strategy not only in NAFLD but also in other liver disorders, such as liver cirrhosis, liver fibrosis and post-ichaemic injury (Edwards et al., 2008; Moal et al., 2002; Ricciardi et al., 2001) that warrants further studies.

Authorship Contribution

Participating in research design: K.Kus, S.Chlopicki

Conducted experiments: K.Kus, M.Walczak, E. Maslak, A.Zakrzewska, A.Gonciarz-Dytman, P.Zabielski, B,Sitek, K.Wandzel, A.Kij A. Chabowski

Contributed new reagents or analytical tools: J.E.Saavedra

Performed data analysis: K.Kus, E.Maslak, R.J. Holland, L.K.Keefer

Wrote or contributed to the writing of the manuscript: K.Kus, S.Chlopicki, E.Maslak, M.Walczak, R.J.Holland, L.K.Keefer

References

An Z, Winnick JJ., Moore MC, Farmer B, Smith M, Irimia JM, Roach PJ, Cherrington AD (2012) A cyclic guanosine monophosphate-dependent pathway can regulate net hepatic glucose uptake in vivo. *Diabetes* 61(10): 2433–2441.

Baranowski M, Blachnio-Zabielska AU, Zabielski P, Harasim E, Harasiuk D, Chabowski A, Gorski J (2013) Liver X receptor agonist T0901317 enhanced peroxisome proliferator-activated receptor-delta expression and fatty acid oxidation in rat skeletal muscle. *J Physiol Pharmacol* 64(3): 289–297.

Carnovale CE, Ronco MT (2012) Role of nitric oxide in liver regeneration. *Ann Hepatol* 11(5): 636–647.

Chakrapani H, Showalter BM, Kong L, Keefer LK, Saavedra JE (2007) V-PROLI/NO, a prodrug of the nitric oxide donor, PROLI/NO. *Org Lett* 9(17): 3409–3412.

Cook S, Hugli O, Egli M, Vollenweider P, Burcelin R, Nicod P, Thorens B, Scherrer U (2003) Clustering of cardiovascular risk factors mimicking the human metabolic syndrome X in eNOS null mice. *Swiss Med Wkly* 133(25-26): 360–363.

De Oliveira CPMS, Simplicio FI, de Lima VMR, Yuahasi K, Lopasso FP, Alves VAF, Abdalla DSP, Carrilho, FJ, Laurindo, FRM, de Oliveira MG (2006) Oral administration of S-nitroso-N-acetylcysteine prevents the onset of non alcoholic fatty liver disease in rats. *World J Gastroenterol* 12(12): 1905–1911.

DeLeve LD (2008) Sinusoidal Obstruction Syndrome *Gastroenterol Hepatol* 4(2), 101–103.

DeLeve LD, Wang X, Kanel GC, Ito Y, Bethea NW, McCuskey MK, Tokes ZA, Tsai J McCuskey RS (2003) Decreased hepatic nitric oxide production contributes to the development of rat sinusoidal obstruction syndrome. *Hepatology* 38(4): 900–908.

Ding X, Kaminsky LS (2003) Human extrahepatic cytochromes P450: function in xenobiotic metabolism and tissue-selective chemical toxicity in the respiratory and gastrointestinal tracts. *Annu Rev Pharmacol Toxicol* 43: 149–173.

Duplain H, Burcelin R, Sartori C, Cook S, Egli M, Lepori M, Vollenweider P, Padrazzini T, Nicod P, Thorens B, Scherrer U (2001) Insulin Resistance, Hyperlipidemia, and Hypertension in Mice Lacking Endothelial Nitric Oxide Synthase. *Circulation* 104(3): 342–345.

Edwards C, Feng H-Q, Reynolds C, Mao L, Rockey DC (2008) Effect of the nitric oxide donor V-PYRRO/NO on portal pressure and sinusoidal dynamics in normal and cirrhotic mice. *Am J Physiol Gastrointest Liver Physiol* 294(6): G1311–1317.

Erion MD, van Poelje PD, Mackenna DA, Colby TJ, Montag AC, Fujitaki JM, Linemeyer DL, Bullough DA (2005) Liver-targeted drug delivery using HepDirect prodrugs. *J Pharmacol Exp Ther* 312(2): 554–560.

Förstermann U, Sessa WC (2012) Nitric oxide synthases: regulation and function. *Eur Heart J* 33(7): 829–837.

Gong P, Cederbaum AI, Nieto N (2004) The Liver-Selective Nitric Oxide Donor O2 -Vinyl 1- (pyrrolidin-1-yl)diazen-1-um-1,2-diolate (V-PYRRO/NO) Protects HEPG2 Cells against Cytochrome P450 2E1-Dependent Toxicity. *Mol Pharmacol* 65(1): 130–138.

González R, Cruz A, Ferrín G, López-Cillero P, Fernández-Rodríguez R, Briceño J, Gómez MA, Rufián S, De la Malta M, Martínez-Ruiz A, Martin JJG, Muntané J (2011) Nitric oxide mimics transcriptional and post-translational regulation during α-tocopherol cytoprotection against glycochenodeoxycholate-induced cell death in hepatocytes. *J Hepatol* 55(1): 133–144.

Gouill ELe, Jimenez M, Binnert C, Jayet P, Thalmann S, Nicod P, Scherrer U, Vollenweider P (2007) Endothelial Nitric Oxide Synthase (eNOS) Knockout Mice Have Defective Mitochondrial B-Oxidation. *Diabetes*, 56: 2690–2696.

Han H K, Amidon GL (2000) Targeted prodrug design to optimize drug delivery. *AAPS PharmSci* 2(1): E6.

Holownia A, Jablonski J, Skiepko A, Mroz R, Sitko E, Braszko JJ (2009) Ruthenium red protects HepG2 cells overexpressing CYP2E1 against acetaminophen cytotoxicity. *Naunyn-Schmiedebergs Arch Pharmacol* 379(1): 27–35.

Hong SY, Borchert GL, Maciag AE, Nandurdikar RS, Saavedra JE, Keefer LK, Phang JM, Chakrapani H (2010) The Nitric Oxide Prodrug V-PROLI/NO Inhibits Cellular Uptake of Proline. *ACS Med Chem Lett* 1(8): 386–389.

Hu LS, George J, Wang, JH (2013) Current concepts on the role of nitric oxide in portal hypertension. *World J Gastroenterol* 19(11): 1707–1717.

Huttunen KM, Mähönen N, Raunio H, Rautio J (2008) Cytochrome P450-activated prodrugs: targeted drug delivery. *Curr Med Chem* 15(23): 2346–2365.

Ijaz S, Yang W, Winslet MC, Seifalian AM (2005) The role of nitric oxide in the modulation of hepatic microcirculation and tissue oxygenation in an experimental model of hepatic steatosis. *Microvasc Res* 70(3): 129–136.

Inami K, Nims RW, Srinivasan A, Citro ML, Saavedra JE, Cederbaum AI, Keefer LK (2006) Metabolism of a liver-selective nitric oxide-releasing agent, V-PYRRO/NO, by human microsomal cytochromes P450. *Nitric Oxide* 14(4): 309–315.

Jobgen W, Meininger CJ, Jobgen SC, Li P, Lee M-J, Smith SB, Spencer TE, Fried SK, Wu G (2009) Dietary L-arginine supplementation reduces white fat gain and enhances skeletal muscle and brown fat masses in diet-induced obese rats. *J Nutr* 139(2): 230–237.

Jobgen WS, Fried SK, Fu WJ, Meininger CJ, Wu G (2006) Regulatory role for the arginine-nitric oxide pathway in metabolism of energy substrates. *J Nutr Biochem* 17(9): 571–588.

Kim Y, Chung H, Simmons RL, Billiar TR (2000) Cellular Non-heme Iron Content Is a Determinant of Nitric Oxide-mediated Apoptosis , Necrosis , and Caspase Inhibition. *J Biol Chem* 275(15): 10954–10961.

Kim YM, Kim TH, Chung HT, Talanian RV, Yin XM, Billiar TR (2000) Nitric oxide prevents tumor necrosis factor alpha-induced rat hepatocyte apoptosis by the interruption of mitochondrial apoptotic signaling through S-nitrosylation of caspase-8. *Hepatology* 32(4 Pt 1): 770–778.

Li C, Liu J, Saavedra JE, Keefer LK, Waalkes MP (2003) The nitric oxide donor, V-PYRRO/NO, protects against acetaminophen-induced nephrotoxicity in mice. *Toxicology* 189(3): 173–180.

Lin J, Schyschka L, Mühl-Benninghaus R, Neumann J, Hao L, Nussler N, Dooley S, Liu L, Stöckle U, Nussler AK, Ehnert S (2012) Comparative analysis of phase I and II enzyme activities in 5 hepatic cell lines identifies Huh-7 and HCC-T cells with the highest potential to study drug metabolism. *Arch Toxicol* 86(1): 87–95.

Liu J, He Y-Y, Chignell CF, Clark J, Myers P, Saavedra JE, Waalkes MP (2005) Limited protective role of V-PYRRO/NO against cholestasis produced by alpha-naphthylisothiocyanate in mice. *Biochem Pharmacol* 70(1): 144–151.

Liu J, Li C, Waalkes MP, Clark J, Myers P, Saavedra JE, Keefer LK (2003) The nitric oxide donor, V-PYRRO/NO, protects against acetaminophen-induced hepatotoxicity in mice. *Hepatology* 37(2): 324–333.

Liu J, Qu W, Saavedra JE, Waalkes MP (2004) The nitric oxide donor, O2-vinyl 1-(pyrrolidin-1-yl)diazen-1-ium-1,2-diolate (V-PYRRO/NO), protects against cadmium-induced hepatotoxicity in mice. *J Pharmacol Exp Ther* 310(1): 18–24.

Liu J, Saavedra JE, Lu T, Song J-G, Clark J, Waalkes MP, Keefer LK (2002) O(2)-Vinyl 1-(pyrrolidin-1-yl)diazen-1-ium-1,2-diolate protection against D-galactosamine/endotoxin-induced hepatotoxicity in mice: genomic analysis using microarrays. *J Pharmacol Exp Ther* 300(1): 18–25.

Liu J, Waalkes MP (2005) Nitric oxide and chemically induced hepatotoxicity: beneficial effects of the liver-selective nitric oxide donor, V-PYRRO/NO. *Toxicology* 208(2): 289–297.

Lowry OH, Rosebrough NJ, Farr AL, Randall RJ (1951) Protein Measurement With the Folin Phenol Reagent. J Biol Chem 193: 265–275.

Lutz SZ, Hennige AM, Feil S, Peter A, Gerling A, Machann J, Kröber SM, Rath M, Schürmann A, Weigert C, Häring H-U, Feil R (2011) Genetic ablation of cGMP-dependent protein kinase type I causes liver inflammation and fasting hyperglycemia. *Diabetes* 60(5): 1566–1576.

Maslak E, Zabielski P, Kochan K, Kus K, Jasztal A, Sitek B, Proniewski B, Wojcik T, Gula K, Kij A, Walczak M, Baranska M, Chabowski A, Holland RJ, Saavedra JE, Keefer LK, Chlopicki S (2015) The liver-selective NO donor, V-PYRRO/NO, protects against liver steatosis and improves postprandial glucose tolerance in mice fed high fat diet. *Biochem Pharmacol* 93(3), 389–400.

Nebert DW, Russell DW (2002) Clinical importance of the cytochromes P450. *Lancet* 360(9340): 1155–1162.

Ortiz de Montellano PR. (2013). Cytochrome P450-activated prodrugs. *Future Med Chem* 5(2): 213–228.

Paine MF, Hart HL, Ludington SS, Haining RL, Rettie AE, Zeldin DC (2006) The human intestinal cytochrome P450 " pie " *Drug Metab Dispos* 34(5): 880–886.

Pavek P, Dvorak Z (2008) Xenobiotic-induced transcriptional regulation of xenobiotic metabolizing enzymes of the cytochrome P450 superfamily in human extrahepatic tissues. *Curr Drug Metab* 9(2): 129–143.

Pawłowska M, Augustin E (2011) Systemy ekspresyjne białek cytochromu P450 w badaniach in vitro metabolizmu leków Expression systems of cytochrome P450 proteins in studies of drug metabolism in vitro. *Postępy Hig Med Dosw* 65: 367–376.

Peter F (1992) Characterization of human cytochrome P450. *FASEB J* 6(2): 745–748.

Pfeifer A, Kilić A, Hoffmann LS (2013) Regulation of metabolism by cGMP. *Pharmacol Ther* 140(1): 81–91.

Qu W, Liu J, Dill AL, Saavedra JE, Keefer LK, Waalkes MP (2010) V-PROLI/NO, a Nitric Oxide DonorProdrug, Protects Liver Cells from Arsenic-Induces Toxicity. *Cancer Sci* 100(3): 382–388.

Qu W, Liu J, Fuquay R, Saavedra JE, Keefer LK, Waalkes MP (2007) The nitric oxide prodrug, V-PYRRO/NO, mitigates arsenic-induced liver cell toxicity and apoptosis. *Cancer Lett* 256(2): 238–245.

Qu W, Liu J, Fuquay R, Shimoda R, Sakurai T, Saavedra JE, Keefer LK, Waalkes MP (2005) The nitric oxide prodrug, V-PYRRO/NO, protects against cadmium toxicity and apoptosis at the cellular level. *Nitric Oxide* 12(2): 114–120.

Ricardo KFS, Shishido SM, de Oliveira MG, Krieger MH (2002) Characterization of the hypotensive effect of S-nitroso-N-acetylcysteine in normotensive and hypertensive conscious rats. *Nitric Oxide* 7(1): 57–66.

Ricciardi R, Foley DP, Quarfordt SH, Saavedra JE, Keefer LK, Wheeler SM, Donohue SE, Callery MP, Meyers WC (2001) V-PYRRO/NO: an hepato-selective nitric oxide donor improves porcine liver hemodynamics and function after ischemia reperfusion. *Transplantation* 71(2): 193–198.

Rockey DC, Shah V (2004) Nitric oxide biology and the liver: report of an AASLD research workshop. *Hepatology* 39(1): 250–257.

Saavedra JE, Billiar TR, Williams DL, Kim Y, Watkins SC, Keefer LK (1997) Targeting Nitric Oxide (NO) Delivery In Vivo. Design of a Liver-Selective NO Donor Prodrug That Blocks Tumor Necrosin Factor-a-Induced Apoptosis and Toxicity in the Liver. *J Med Chem* 40(13): 1947–1954.

Sadri P, Lautt WW (1999) Blockade of hepatic nitric oxide synthase causes insulin resistance. *Am J Physiol Gastrointest Liver Physiol* 277(1): G101–108.

Sansbury BE, Cummins TD, Tang Y, Hellmann J, Holden CR, Harbeson MA, Chen Y, Patel RP, Spite M, Bhatnagar A, Hill BG (2012) Overexpression of endothelial nitric oxide synthase prevents diet-induced obesity and regulates adipocyte phenotype. *Circ Res* 111(9): 1176–1189.

Siriussawakul A (2010) Role of nitric oxide in hepatic ischemia-reperfusion injury. *World Gastroenterol* 16(48): 6079-6086.

Stinson SF, House T, Bramhall C, Saavedra JE, Keefer LK, Nims RW (2002) Plasma pharmacokinetics of a liver-selective nitric oxide-donating diazeniumdiolate in the male C57BL/6 mouse. *Xenobiotica* 32(4): 339–347.

Tateya S, Rizzo NO, Handa P, Cheng AM, Morgan-Stevenson V, Daum G, Clowes AW, Morton GJ, Schwartz MW, Kim F (2011) Endothelial NO/cGMP/VASP signaling attenuates Kupffer cell activation and hepatic insulin resistance induced by high-fat feeding. *Diabetes* 60(11): 2792–2801.

Testa B (2009) Prodrugs: bridging pharmacodynamic/pharmacokinetic gaps. *Curr Opin Chem Biol* 13(3): 338–344.

Van den Berg SA, Guigas B, Bijland S, Ouwens M, Voshol PJ, Frants RR, Havekes LM, Romijn JA, van Dijk KW (2010) High levels of dietary stearate promote adiposity and deteriorate hepatic insulin sensitivity. *Nutr Metab* 7: 24.

Warensjö E, Risérus U, Vessby B (2005) Fatty acid composition of serum lipids predicts the development of the metabolic syndrome in men. *Diabetologia* 48(10): 1999–2005.

Westerink WMA, Schoonen WGEJ (2007) Cytochrome P450 enzyme levels in HepG2 cells and cryopreserved primary human hepatocytes and their induction in HepG2 cells. *In Vitro Toxicol* 21(8): 1581–1591.

Wierzbicki M, Chabowski A, Zendzian-Piotrowska M, Harasim E, Górski J (2009) Chronic, in vivo, PPARalpha activation prevents lipid overload in rat liver induced by high fat feeding. *Adv Med Sci* 54(1): 59–65.

Zabielski P, Baranowski M, Błachnio-Zabielska A, Zendzian-Piotrowska M, Górski J (2010) The effect of high-fat diet on the sphingolipid pathway of signal transduction in regenerating rat liver. *Prostaglandins Other Lipid Mediat* 93: 75–83.

Zawilska JB, Wojcieszak J, Olejniczak AB (2013) Prodrugs: a challenge for the drug development. *Pharmacol Rep* 65(1): 1–14.

Footnotes

This work was supported by the Polish National Science Center [DEC-2013/11/N/NZ7/00749]; and the European Union from the resources of the European Regional Development Fund under the Innovative Economy Programme, grant coordinated by JCET-UJ,. [POIG.01.01.02-00-069/09].

Figure legends

Figure1. Structures of the studied NO-donors V-PYRRO/NO and V-PROLI/NO.

Figure 2. Representative pictures liver sections stained with (A) H&E, (B) one step Gomorie's trichromeand (C) OilRed O. Liver fat content calculated from OilRed O pictures (D), liver triglyceride (TG) concentration (E) and PUFA/SFA ratio (F) in the liver of mice. The glucose tolerance curve (G) and the area under the curve of blood glucose concentration versus time (AUC) (H). Values are means ± SEM (n=6). Values with different superscript letters within each animal group are significantly different ($p \leq 0.05$). HF: high fat group; HF+V-PYRRO/NO: high fat group treated with V-PYRRO/NO; HF+V-PROLI/NO: high fat group treated with V-PROLI/NO.

Figure 3. Comparison of plasma pharmacokinetic profiles of V-PYRRO/NO and V-PROLI/NO (A) after *i.v.* and *i.p.* administration in mice, and NO_2^-, NO_3^- concentrations in plasma after *i.v.* administration of each compound (B, C). Values are expressed as mean ± SEM, n=3 for *i.p.* and n=4 for *i.v.* administration.

Figure. 4. Calculated differences for V-PYRRO/NO and V-PROLI/NO concentrations between inlet and outlet effluent samples following perfusion with 10 µM (A) and 50 µM (B) of compound. Fraction of dose that was eliminated unchanged by the kidney (C). Values are expressed as mean ± SEM, statistical significance * $p<0.05$, ** $p<0.01$, n=4 for isolated, perfused mouse liver experiments, and n = 7 for renal elimination evaluation.

Figure 5. Michaelis-Menten plots of the enzyme kinetics of V-PYRRO/NO and V-PROLI/NO in rat liver microsomes (A). The effect of selective P450 inhibitors on V-PYRRO/NO and V-PROLI/NO (50µM) metabolism in rat liver microsomes (B). Values are shown as mean percentage ± SEM (n=3 for furafilline, sulpaphenazole, N-benzilnirvanol and ketoconazole; n=6 for disulfiram).

DMD Fast Forward. Published on April 13, 2015 as DOI: 10.1124/dmd.115.063388
This article has not been copyedited and formatted. The final version may differ from this version.

Table 1. Pharmacokinetic parameters of V-PYRRO/NO and V-PROLI/NO after *i.v.* and *i.p.* administration in control mice.

Parameter	V-PYRRO/NO		V-PROLI/NO	
	Intravenous	Intraperitoneal	Intravenous	Intraperitoneal
C_o[µM]	41.5	-	222.48	-
$AUC_{0\rightarrow\infty}$ [µM*min]	218.62	60.9	5669.26	2895.27
MRT [min]	6	7.7	27.87	28.57
C_{max} [µM]	-	7.93	-	79.57
t_{max} [min]	-	5	-	10
V_{ss} [L/kg]	0.88	-	0.149	-
Cl [L/min/kg]	0.146	-	0.0053	-
F [%]	-	27.85	-	51.07

Figure 1

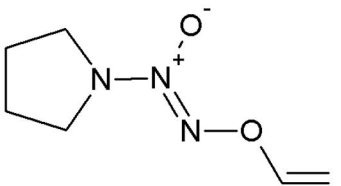

V-PYRRO/NO

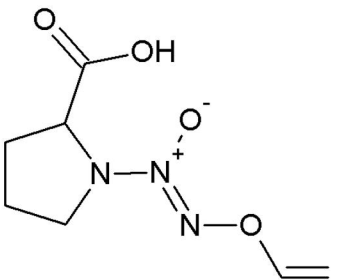

V-PROLI/NO

Figure 2

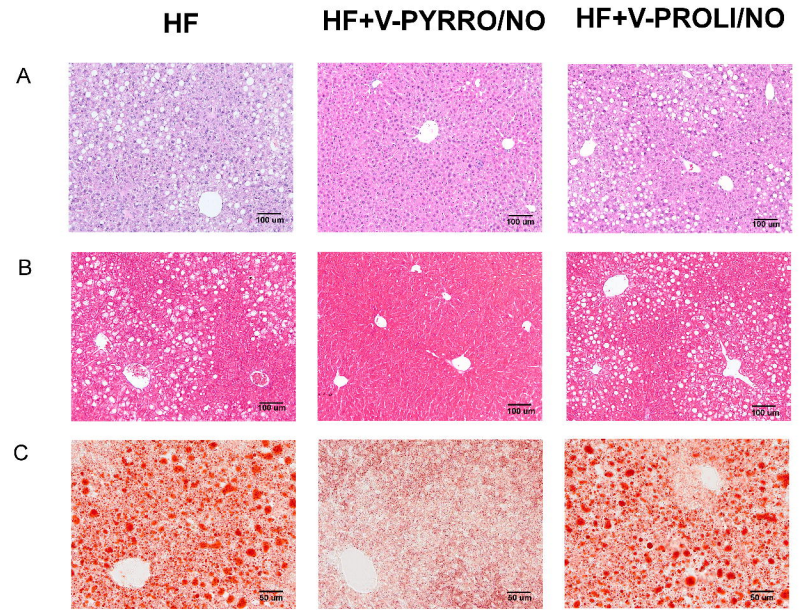
HF
HF+V-PYRRO/NO
HF+V-PROLI/NO
A
B
C
100 um
50 um

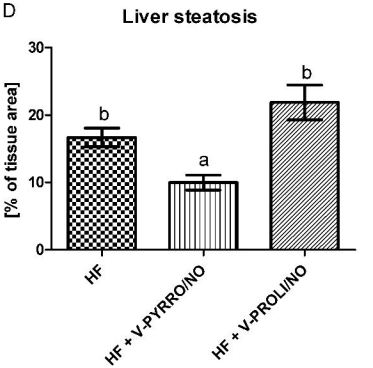
D
Liver steatosis
[% of tissue area]
30
20
10
0
b
a
b
HF
HF + V-PYRRO/NO
HF + V-PROLI/NO

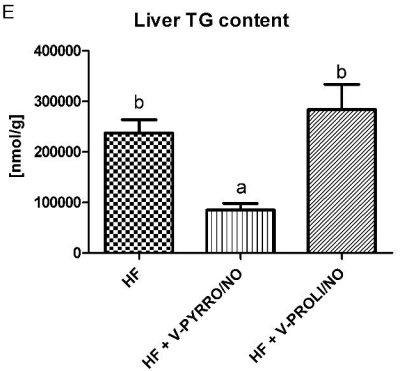
E
Liver TG content
[nmol/g]
400000
300000
200000
100000
0
b
a
b
HF
HF + V-PYRRO/NO
HF + V-PROLI/NO

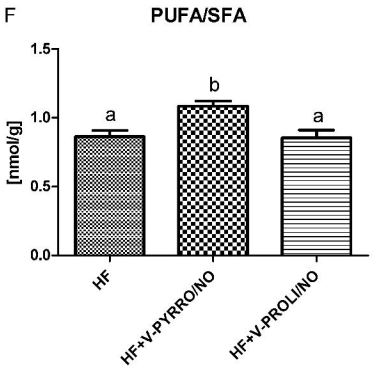
F
PUFA/SFA
[nmol/g]
1.5
1.0
0.5
0.0
a
b
a
HF
HF+V-PYRRO/NO
HF+V-PROLI/NO

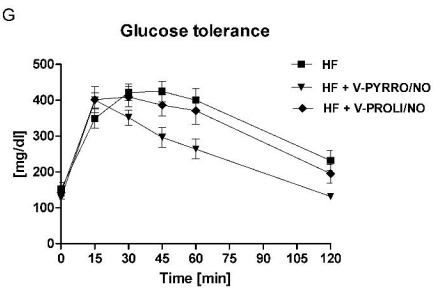
G
Glucose tolerance
[mg/dl]
500
400
300
200
100
0
0
15
30
45
60
75
90
105
120
Time [min]
HF
HF + V-PYRRO/NO
HF + V-PROLI/NO

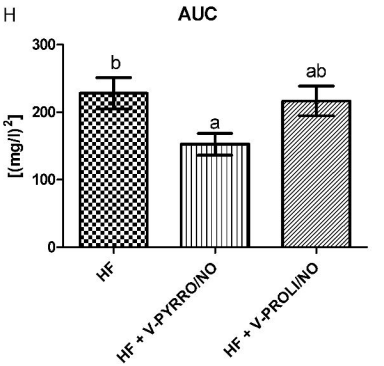
H
AUC
[(mg/l)²]
300
200
100
0
b
a
ab
HF
HF + V-PYRRO/NO
HF + V-PROLI/NO

Figure 3

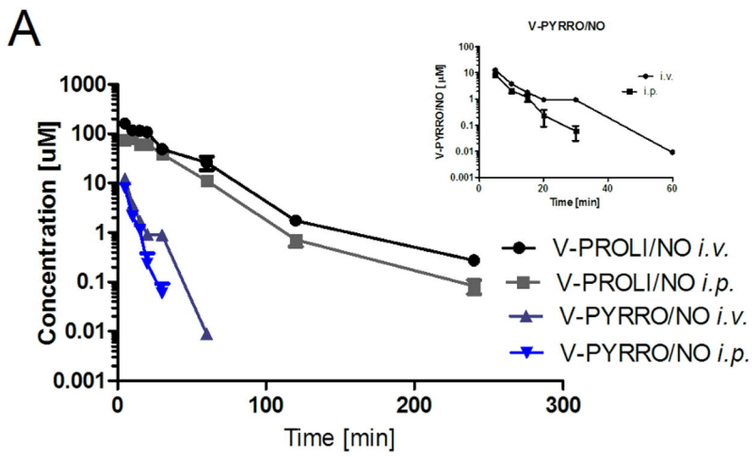
A
V-PYRRO/NO
i.v.
i.p.
Time [min]
Concentration [uM]
Time [min]
V-PROLI/NO i.v.
V-PROLI/NO i.p.
V-PYRRO/NO i.v.
V-PYRRO/NO i.p.

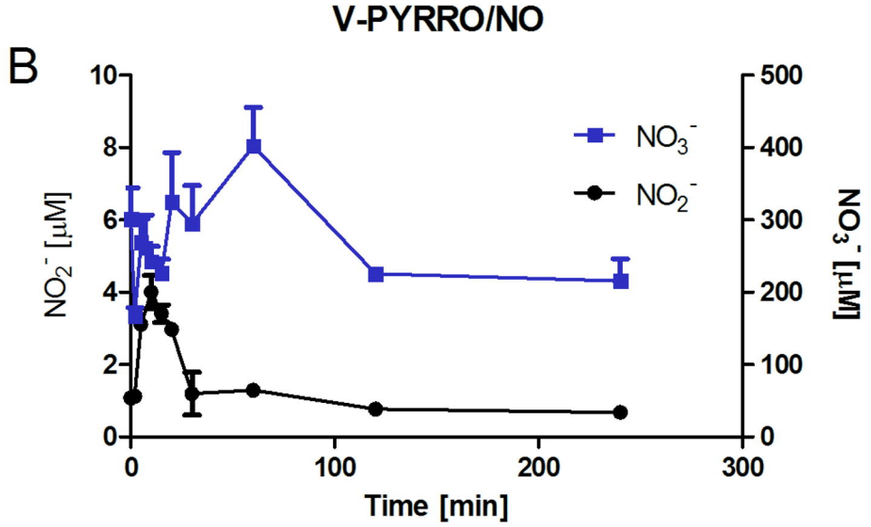
B
V-PYRRO/NO
NO3-
NO2-
NO2- [µM]
NO3- [µM]
Time [min]

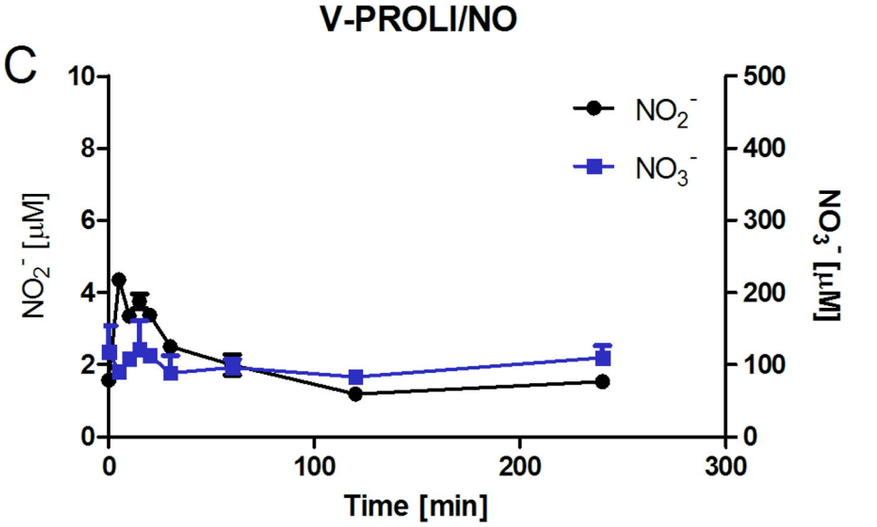
C
V-PROLI/NO
NO2-
NO3-
NO2- [µM]
NO3- [µM]
Time [min]

Figure 4

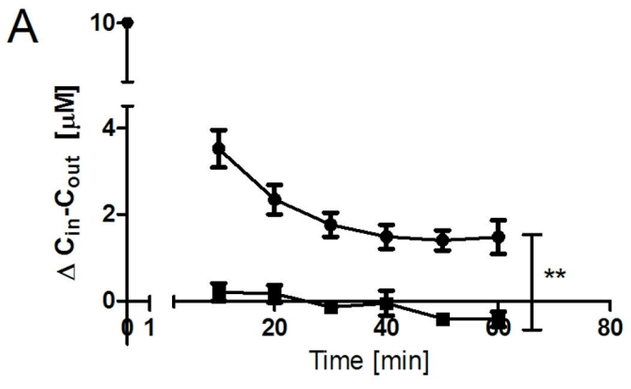

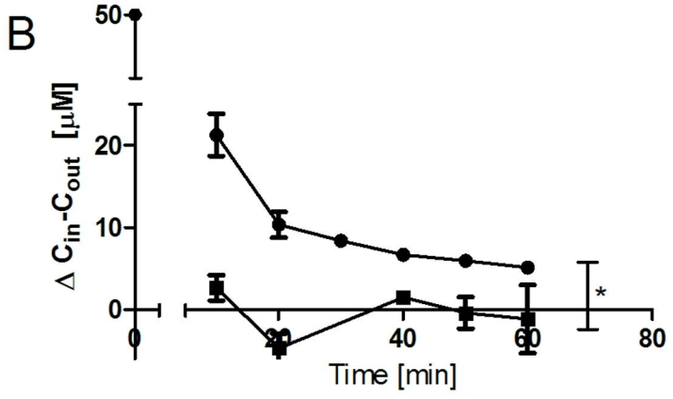

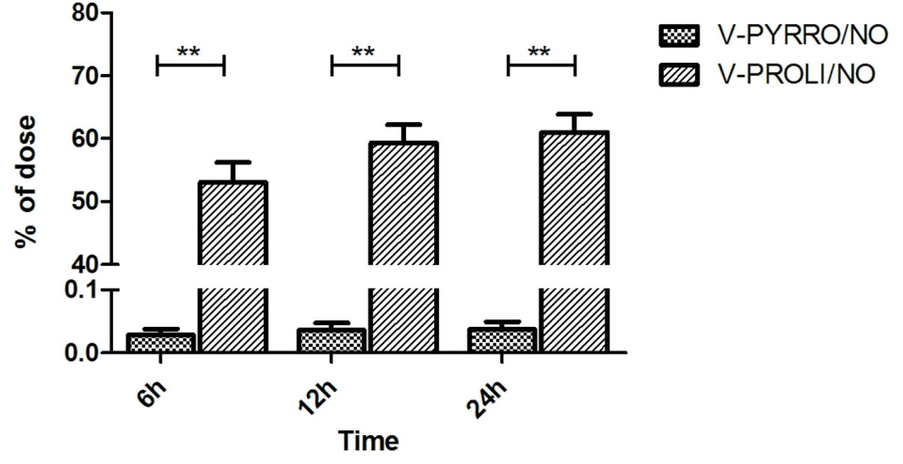

V-PYRRO/NO V-PROLI/NO

Figure 5

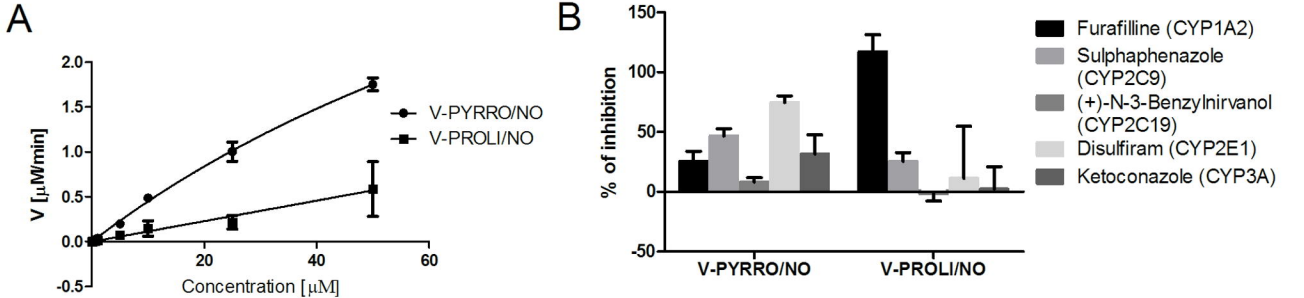
A
2.0
1.5
1.0
0.5
0.0
-0.5
V [μM/min]
20
40
60
Concentration [μM]
V-PYRRO/NO
V-PROLI/NO
B
150
100
50
0
-50
% of inhibition
V-PYRRO/NO
V-PROLI/NO
Furafilline (CYP1A2)
Sulphaphenazole (CYP2C9)
(+)-N-3-Benzylnirvanol (CYP2C19)
Disulfiram (CYP2E1)
Ketoconazole (CYP3A)